

# Precise QCD predictions for the production of dijet final states in deep inelastic scattering

James Currie<sup>a,c</sup>, Thomas Gehrmann<sup>b,c</sup>, Jan Niehues<sup>b</sup>

<sup>a</sup>*Institute for Particle Physics Phenomenology, Department of Physics, University of Durham, Durham, DH1 3LE, UK*

<sup>b</sup>*Department of Physics, University of Zürich, Winterthurerstrasse 190, CH-8057 Zürich, Switzerland*

<sup>c</sup>*Kavli Institute for Theoretical Physics, University of California, Santa Barbara, CA 93106, USA*

The production of two-jet final states in deep inelastic scattering is an important QCD precision observable. We compute it for the first time to next-to-next-to-leading order (NNLO) in perturbative QCD. Our calculation is fully differential in the lepton and jet variables and allows one to impose cuts on the jets both in the laboratory and the Breit frame. We observe that the NNLO corrections are moderate in size, except at kinematical edges, and that their inclusion leads to a substantial reduction of the scale variation uncertainty on the predictions. Our results will enable the inclusion of deep inelastic dijet data in precision phenomenology studies.

PACS numbers: 13.87.-a, 13.60.Hb, 12.38Bx

Our understanding of the inner structure of the proton has been shaped through a long series of deep-inelastic lepton-nucleon experiments, which have established the partonic structure of the proton and provided precision measurements of parton distribution functions [1]. Specific combinations of the quark distributions can be probed in inclusive deep inelastic scattering (DIS), where the gluon distribution only enters indirectly as a correction and through scaling violations. A direct probe of the gluon distribution, which is less well constrained than the quark distributions, requires the selection of specific hadronic final states in deep inelastic scattering [2], such as heavy quarks or jets.

Dijet final states in DIS are formed [3] through the two basic scattering processes  $\gamma^* q \rightarrow qg$  and  $\gamma^* g \rightarrow q\bar{q}$ , which vary in relative importance depending on the kinematical region. Especially at low invariant masses of the dijet system, the gluon-induced process is largely dominant. The interplay of lepton and dijet kinematics in this region allows the gluon distribution to be probed over a substantial range. The same process also provides a direct measurement of the strong coupling constant  $\alpha_s$ .

The DESY HERA electron-proton collider provided a large data set of hadronic final states in DIS at  $\sqrt{s} = 319$  GeV. Dijet final states have been measured to high precision over a large kinematical range by the H1 [4–6] and ZEUS [7, 8] experiments, that have also used these measurements in the determination of the strong coupling constant. The reconstruction of jets is performed in the Breit frame, defined by the direction of the virtual photon and incoming proton, while the jet rapidity coverage is limited by the detector’s geometry in the laboratory frame. Consequently, the definition of the fiducial phase space used in a jet measurement typically combines information from both frames.

The interpretation of HERA data on dijet production in DIS relies at present on theoretical predictions at next-to-leading order (NLO) in perturbative QCD [9–11]. The uncertainty associated with the NLO predictions (as esti-

mated through the variation of renormalization and factorization scales) is the main limitation to precision studies based on these data. In particular, they can not be included in a consistent manner in state-of-the-art determinations of parton distributions [12–15], which typically require their input data to be described at next-to-next-to-leading order (NNLO) QCD accuracy.

In this letter, we present the first calculation of the next-to-next-to-leading order (NNLO) QCD prediction to dijet production in DIS. The QCD corrections at this order involve three types of scattering amplitudes: the two-loop amplitudes for two-parton final states [16], the one-loop amplitudes for three-parton final states [17] and the tree-level amplitudes for four-parton final states [18]. The contribution from each partonic final state multiplicity contains infrared divergences from soft and collinear real radiation and from virtual particle loops; these infrared singularities cancel only once the different multiplicities are summed together for any infrared-safe final state definition [19]. To implement the different contributions into a numerical program, a procedure for the extraction of all infrared singular configurations from each partonic multiplicity is needed. Several methods have been developed for this task at NNLO: sector decomposition [20],  $q_T$ -subtraction [21], antenna subtraction [22], sector-improved residue subtraction [23],  $N$ -jettiness subtraction [24] and colorful subtraction [25].

Our calculation is based on the antenna subtraction method [22], which constructs the subtraction terms for the real radiation processes out of antenna functions that encapsulate all color-ordered unresolved parton emission in between a pair of hard radiator partons, multiplied with reduced matrix elements of lower partonic multiplicity. By factorizing the final state phase space accordingly, it is possible to analytically integrate the antenna functions to make their infrared pole structure explicit, such that the integrated subtraction terms can be combined with the virtual corrections to yield a finite result. In the case of jet production in deep inelastic scattering, we

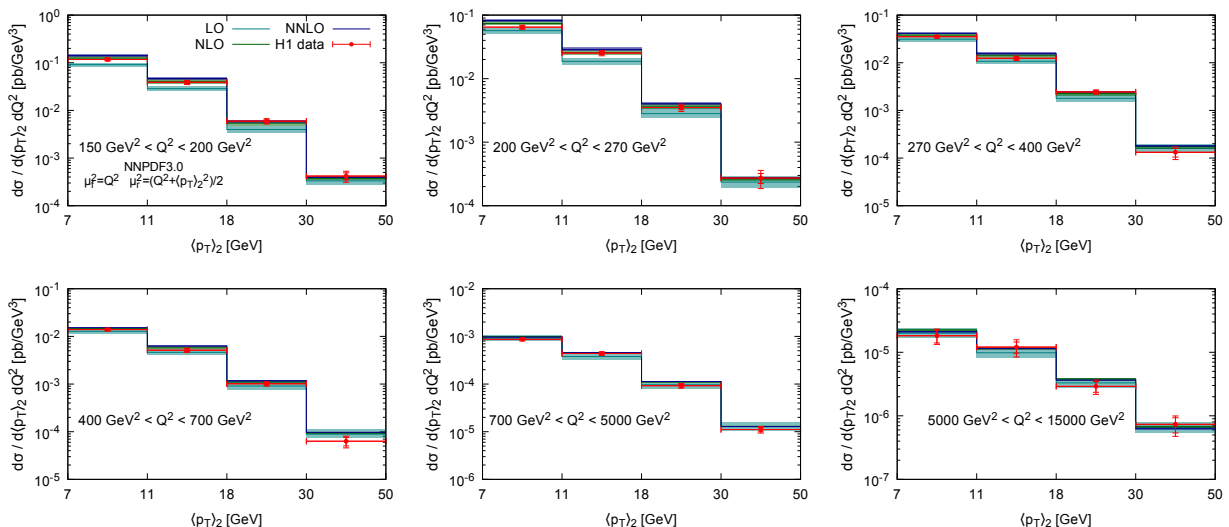


FIG. 1. Inclusive dijet production in deep inelastic scattering as function of the average transverse momentum of the two leading jets in the Breit frame at LO, NLO, NNLO, compared to data from the H1 collaboration [6].

need to use antenna functions with both hard radiators in the final state [22] and with one radiator in the initial and one in the final state [27]. The combination of real radiation contributions and unintegrated antenna subtraction terms is numerically finite in all infrared limits, such that all parton-level contributions to two-jet final states at NNLO can be implemented into a numerical program (parton-level event generator). This program can then incorporate the jet algorithm used in the experimental measurement as well as any type of event selection cuts. A substantial part of the infrastructure of our program is common to other NNLO calculations of jet production observables within the antenna subtraction method [28–32], which are all part of a newly developed code named NNLOJET. To validate our implementation of the tree-level and one-loop matrix elements, we compared the NLO predictions for dijet and trijet production against SHERPA [33] (in DIS kinematics [34]), which uses OpenLoops [35] to automatically generate the one-loop contributions at NLO. The antenna subtraction is then verified by testing the convergence of subtraction terms and matrix elements in all unresolved limits (as documented for example in [36]) and by the infrared pole cancellation between the integrated subtraction terms and the two-loop matrix elements.

As a first application of our calculation, we consider the recent measurement by the H1 collaboration [6] of dijet production in DIS at high virtuality  $Q^2$ . The measurement was performed on data taken at the DESY HERA electron proton collider at a centre-of-mass energy of  $\sqrt{s} = 319$  GeV. Deep inelastic scattering events are selected by requiring the range of lepton scattering variables: exchanged boson virtuality  $150 \text{ GeV}^2 < Q^2 < 15000 \text{ GeV}^2$  and energy transfer in the proton rest

system  $0.2 < y < 0.7$ . The hadronic final state is boosted to the Breit frame of reference, where the jet clustering is performed using the inclusive hadronic  $k_T$  algorithm [37] with  $E_T$  recombination. To ensure that the jets are contained in the calorimeter coverage, a cut on their pseudorapidity is applied in the HERA laboratory frame:  $-1.0 < \eta_L < 2.5$ . Jets are accepted in the inclusive dijet sample if their transverse momentum in the Breit frame is  $5 \text{ GeV} < p_{T,B} < 50 \text{ GeV}$  and are ordered in this variable. The event is retained if the invariant mass of the two leading jets is  $M_{12} > 16 \text{ GeV}$ . The H1 collaboration provides double differential distributions in  $Q^2$  and either the average transverse momentum of the two leading jets  $\langle p_T \rangle_2 = (p_{T1,B} + p_{T2,B})/2$  or the variable  $\xi_2 = x(1 + M_{12}/Q^2)$  where  $x$  is the Bjorken variable reconstructed from the lepton kinematics. At leading order,  $\xi_2$  can be identified with the proton momentum fraction carried by the parton that initiated the hard scattering process.

The theoretical predictions use the NNPDF3.0 parton distribution functions [14] with  $\alpha_s(M_Z^2) = 0.118$  and are evaluated with default renormalization and factorization scales  $\mu_R = \sqrt{Q^2 + \langle p_T \rangle_2^2}$ ,  $\mu_F = \sqrt{Q^2}$ . The uncertainty on the theoretical prediction from missing higher orders is estimated by varying these scales by a factor between 1/2 and 2. The electromagnetic coupling is also evaluated at a dynamical scale as  $\alpha(Q^2)$  according to QED evolution, with  $\alpha(100 \text{ GeV}^2) = 0.0075683$ . The theoretical predictions are corrected bin-by-bin for hadronization and electroweak effects using the tables provided in [6].

Figure 1 displays the  $\langle p_T \rangle_2$  distribution in six  $Q^2$  bins. For better visibility, the same plots are normalized to the NLO prediction in Figure 2, excluding the LO contribution which is typically considerably below the NLO curve

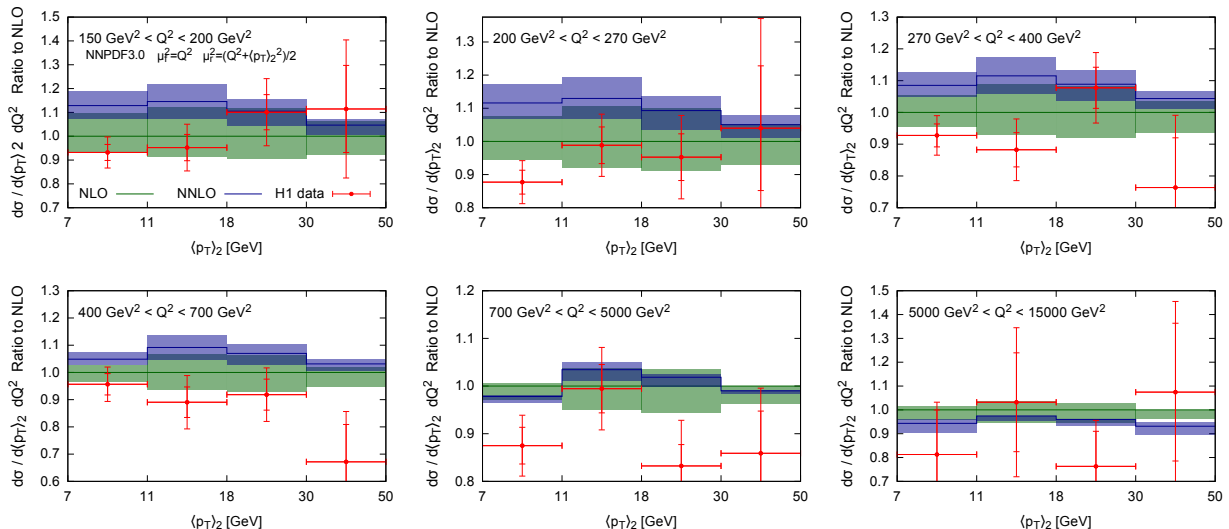


FIG. 2. Inclusive dijet production in deep inelastic scattering as function of the average transverse momentum of the two leading jets in the Breit frame normalized to NLO and compared to data from the H1 collaboration [6].

and is associated with a large error. We observe that for all but the first bins in  $\langle p_T \rangle_2$ , the NNLO predictions are inside the NLO uncertainty band and that their inclusion leads to a substantial reduction of the theory uncertainty to typically 5% or less (especially at high  $Q^2$ ), which is now below the statistical and systematical uncertainty on the experimental data. We observe that the theoretical NNLO predictions tend to be above the experimental data. This feature points to the potential impact that the inclusion of these data could have in a global determination of parton distributions and of the strong coupling constant at NNLO accuracy. The tension between data and NNLO predictions is largest at lower values of  $Q^2$ , where the data is most accurate and the gluon-induced subprocess dominates the dijet production cross section.

The first bins in  $\langle p_T \rangle_2$  display a larger correction, often at the upper boundary of the NLO band, and only a mild reduction in scale uncertainty. They already have very large NLO corrections, typically with a NLO/LO ratio of about 2. This feature can be understood from a sophisticated interplay of the  $M_{12} > 16$  GeV cut with the other jet cuts. The  $M_{12}$  cut forbids a substantial part of the phase space relevant to the first bin in the  $\langle p_T \rangle_2$  distribution to be filled by the leading order process. This results in a perturbative instability [38] starting below  $\langle p_T \rangle_2 = 8$  GeV, which leads to a destabilization of the perturbative series for the first bin.

To further illustrate this issue, we display the  $\xi_2$  distribution in the lowest bin in  $Q^2$  in Figure 3. The same perturbative instability is present, now spread more uniformly over the first two bins. It is more pronounced than in the  $\langle p_T \rangle_2$  distribution due to the fact that an even larger fraction of the phase space is forbidden at leading order, since jets down to  $p_{T,B} = 5$  GeV are accepted in

this distribution, while maintaining the  $M_{12} > 16$  GeV cut. The resulting instability can already be seen in going from LO to NLO, with substantial corrections outside the nominal scale variation band. In the bins with larger  $\xi_2$ , events with low  $M_{12}$  close to the cut are of lower importance, resulting in a better perturbative convergence and a more reliable prediction.

In this letter, we presented the first calculation of dijet production in deep inelastic scattering to NNLO in QCD. Our results are fully differential in the kinematical variables of the final state lepton and the jets. We applied our calculation to the kinematical situation that is relevant to a recent dijet measurement by the H1 collaboration [6]. Except for jet production at low transverse momentum (where the experimental event selection cuts destabilize the perturbative convergence), we observe the NNLO corrections to be moderate in size, and overlapping with the scale uncertainty band of the previously available NLO calculation. Especially at lower  $Q^2$ , the

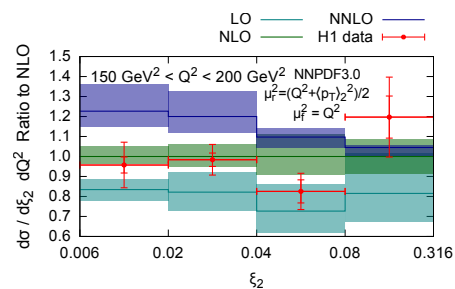


FIG. 3. Inclusive dijet production in deep inelastic scattering as function of  $\xi_2$  normalized to NLO and compared to data from the H1 collaboration [6].

NNLO predictions tend to be above the data, which could provide important new information on the gluon distribution at NNLO. The residual uncertainty on the NNLO results is of the order of 5% or less, and below the errors on the experimental data. Our results enable the inclusion of deep inelastic jet data into precision phenomenology studies of the structure of the proton and of the strong coupling constant.

We would like to thank Nigel Glover, Alexander Huss and Thomas Morgan for many interesting discussions throughout the whole course of this project, Stefan Höche and Marek Schönherr for help with the NLO comparisons against SHERPA and Daniel Britzger for useful clarifications on the H1 jet data. This research was supported in part by the Swiss National Science Foundation (SNF) under contract 200020-162487, in part by the UK Science and Technology Facilities Council as well as by the Research Executive Agency (REA) of the European Union under the Grant Agreement PITN-GA-2012-316704 (“HiggsTools”), the ERC Advanced Grant MC@NNLO (340983) and by the National Science Foundation under grant NSF PHY11-25915.

- 
- [1] R. Devenish and A. Cooper-Sarkar, *Deep inelastic scattering*, Oxford University Press (Oxford, 2004).
- [2] P. Newman, M. Wing, *Rev. Mod. Phys.* **86** (2014) 1037.
- [3] K.H. Streng, T.F. Walsh and P.M. Zerwas, *Z. Phys. C* **2** (1979) 237; R. D. Peccei and R. Rückl, *Nucl. Phys. B* **162** (1980) 125; C. Rumpf, G. Kramer and J. Willrodt, *Z. Phys. C* **7** (1981) 337.
- [4] A. Aktas *et al.* [H1 Collaboration], *Phys. Lett. B* **653** (2007) 134.
- [5] F. D. Aaron *et al.* [H1 Collaboration], *Eur. Phys. J. C* **67** (2010) 1.
- [6] V. Andreev *et al.* [H1 Collaboration], *Eur. Phys. J. C* **75** (2015) 65.
- [7] S. Chekanov *et al.* [ZEUS Collaboration], *Phys. Lett. B* **547** (2002) 164.
- [8] H. Abramowicz *et al.* [ZEUS Collaboration], *Eur. Phys. J. C* **70** (2010) 965.
- [9] E. Mirkes and D. Zeppenfeld, *Phys. Lett. B* **380** (1996) 205.
- [10] D. Graudenz, *Phys. Rev. D* **49** (1994) 3291; hep-ph/9710244.
- [11] Z. Nagy and Z. Trocsanyi, *Phys. Rev. Lett.* **87** (2001) 082001.
- [12] S. Alekhin, J. Blümlein and S. Moch, *Phys. Rev. D* **89** (2014) 054028.
- [13] L.A. Harland-Lang, A.D. Martin, P. Motylinski and R.S. Thorne, *Eur. Phys. J. C* **75** (2015) 204.
- [14] R. D. Ball *et al.*, *JHEP* **1504** (2015) 040.
- [15] S. Dulat *et al.*, *Phys. Rev. D* **93** (2016) 033006.
- [16] L.W. Garland, T. Gehrmann, E.W.N. Glover, A. Koukoutsakis and E. Remiddi, *Nucl. Phys. B* **627** (2002) 107; *Nucl. Phys. B* **642** (2002) 227; T. Gehrmann and E. Remiddi, *Nucl. Phys. B* **640** (2002) 379; T. Gehrmann and E.W.N. Glover, *Phys. Lett. B* **676** (2009) 146.
- [17] E. W. N. Glover and D. J. Miller, *Phys. Lett. B* **396** (1997) 257; Z. Bern, L. J. Dixon, D. A. Kosower and S. Weinzierl, *Nucl. Phys. B* **489** (1997) 3; J. M. Campbell, E. W. N. Glover and D. J. Miller, *Phys. Lett. B* **409** (1997) 503; Z. Bern, L. J. Dixon and D. A. Kosower, *Nucl. Phys. B* **513** (1998) 3.
- [18] K. Hagiwara and D. Zeppenfeld, *Nucl. Phys. B* **313** (1989) 560; F. A. Berends, W. T. Giele and H. Kuijf, *Nucl. Phys. B* **321** (1989) 39; N. K. Falck, D. Graudenz and G. Kramer, *Nucl. Phys. B* **328** (1989) 317.
- [19] G. F. Sterman and S. Weinberg, *Phys. Rev. Lett.* **39** (1977) 1436.
- [20] T. Binoth and G. Heinrich, *Nucl. Phys. B* **693** (2004) 134; C. Anastasiou, K. Melnikov and F. Petriello, *Phys. Rev. D* **69** (2004) 076010.
- [21] S. Catani and M. Grazzini, *Phys. Rev. Lett.* **98** (2007) 222002.
- [22] A. Gehrmann-De Ridder, T. Gehrmann and E.W.N. Glover, *JHEP* **0509** (2005) 056; *Phys. Lett. B* **612** (2005) 49; *Phys. Lett. B* **612** (2005) 36; J. Currie, E. W. N. Glover and S. Wells, *JHEP* **1304** (2013) 066.
- [23] M. Czakon, *Phys. Lett. B* **693** (2010) 259; R. Boughezal, K. Melnikov and F. Petriello, *Phys. Rev. D* **85** (2012) 034025.
- [24] R. Boughezal, C. Focke, X. Liu and F. Petriello, *Phys. Rev. Lett.* **115** (2015) 062002; R. Boughezal, X. Liu and F. Petriello, *Phys. Rev. D* **91** (2015) 094035; J. Gaunt, M. Stahlhofen, F. J. Tackmann and J. R. Walsh, *JHEP* **1509** (2015) 058.
- [25] G. Somogyi and Z. Trocsanyi, *JHEP* **0808** (2008) 042; V. Del Duca, C. Duhr, A. Kardos, G. Somogyi and Z. Trocsanyi, arXiv:1603.08927.
- [26] A. Daleo, T. Gehrmann and D. Maitre, *JHEP* **0704** (2007) 016.
- [27] A. Daleo, A. Gehrmann-De Ridder, T. Gehrmann and G. Luisoni, *JHEP* **1001** (2010) 118.
- [28] A. Gehrmann-De Ridder, T. Gehrmann, E.W.N. Glover and G. Heinrich, *JHEP* **0711** (2007) 058; *Comput. Phys. Commun.* **185** (2014) 3331.
- [29] A. Gehrmann-De Ridder, T. Gehrmann, E.W.N. Glover and J. Pires, *Phys. Rev. Lett.* **110** (2013) 162003; J. Currie, A. Gehrmann-De Ridder, E.W.N. Glover and J. Pires, *JHEP* **1401** (2014) 110.
- [30] G. Abelof, A. Gehrmann-De Ridder and I. Majer, *JHEP* **1512** (2015) 074.
- [31] X. Chen, T. Gehrmann, E.W.N. Glover and M. Jaquier, *Phys. Lett. B* **740** (2015) 147.
- [32] A. Gehrmann-De Ridder, T. Gehrmann, E.W.N. Glover, A. Huss and T.A. Morgan, arXiv:1507.02850; arXiv:1605.04295.
- [33] T. Gleisberg, S. Höche, F. Krauss, M. Schönherr, S. Schumann, F. Siegert and J. Winter, *JHEP* **0902** (2009) 007.
- [34] T. Carli, T. Gehrmann and S. Höche, *Eur. Phys. J. C* **67** (2010) 73.
- [35] F. Cascioli, P. Maierhöfer and S. Pozzorini, *Phys. Rev. Lett.* **108** (2012) 111601.
- [36] E.W.N. Glover and J. Pires, *JHEP* **1006** (2010) 096; A. Gehrmann-De Ridder, E.W.N. Glover and J. Pires, *JHEP* **1202** (2012) 141.
- [37] S. Catani, Y.L. Dokshitzer, M.H. Seymour and B.R. Webber, *Nucl. Phys. B* **406** (1993) 187; G.P. Salam, *Eur. Phys. J. C* **67** (2010) 637.
- [38] S. Catani and B.R. Webber, *JHEP* **9710** (1997) 005.